

Identification of Damaged Areas due to the 2006 Central Java, Indonesia Earthquake Using Satellite Optical Images

Hiroyuki Miura

Center for Urban Earthquake
Engineering,
Tokyo Institute of Technology
Yokohama, Japan
hmiura@enveng.titech.ac.jp

Fumio Yamazaki

Dept. of Urban Environment Systems,
Chiba University
Chiba, Japan
yamazaki@tu.chiba-u.ac.jp

Masashi Matsuoka

Earthquake Disaster Mitigation
Research Center, NIED
Kobe, Japan
matsuoka@edm.bosai.go.jp

Abstract— In order for efficient post disaster management, it is important to develop a methodology to capture affected areas from remote sensing data. In this paper, the areas damaged by the 2006 Central Java earthquake are identified from the high-resolution satellite images. Based on the field survey for the spectral reflectance of surface materials, the image classification technique is applied to post-earthquake QuickBird images to detect the areas covered with bricks (damaged buildings) and the areas covered with roof tiles (undamaged buildings). The distribution of the building damage is evaluated by computing Damage Index from the classified images. The severely damaged areas are distributed not only in Bantul and Imogiri, located near the epicenter, but also in Gantiwarno, the southern part of Klaten located 20-30km away from the epicenter. The distribution of the DI is compared with the damage statistics by the field survey. The result shows that the DI almost agrees with the severe damage ratio.

I. INTRODUCTION

The 2006 Central Java earthquake (Mw6.3) occurred in the state of Yogyakarta, Indonesia on May 27, 2006. More than 5,700 human lives were lost, 36,000 people were injured due to the earthquake. Approximately 140,000 houses were collapsed and 200,000 were damaged. After the earthquake, the field survey of the affected areas had been conducted by many researchers to investigate the distribution of the damage and their causes. However, the identification of the damaged area by the field survey is time-consuming in case of a large-scale disaster. For early rescue activities and efficient post disaster management, it is important to develop a methodology to quickly identify the distribution of the damaged areas.

Remote sensing data observed from satellites would be useful to detect the affected areas since the surface condition of vast area can be identified from the images. Recently, commercial high-resolution satellite images, such as QuickBird (QB) or IKONOS, are easily available. After the 2006 Central Java earthquake, the International charter of "Space and major disaster" [1] had activated to obtain satellite remote sensing images of the severely damaged area. Especially, UNOSAT [2] had published the damage distribution map estimated from the high-resolution satellite images on their web site. Figure 1

shows the damage distribution estimated by UNOSAT overlaid on the satellite ASTER image. The map is very useful to grasp the distribution of the building damage in the early-stage of the post disaster. The map shows the building damage is concentrated in the south of Yogyakarta, such as Bantul and Imogiri. However, according to the damage statistics [3], the building damage is distributed to the east of Yogyakarta, such as Gantiwarno in Klaten where the damage is not described in the map. This is because the images in the southern part of Klaten are not used in the UNOSAT map.

The visual interpretation technique was applied to identify the damage are in the UNOSAT map. The technique requires great demand of time and labor, although it can provide the distribution of the reliable building damage. Therefore, more efficient technique is necessary for more quick identification of the building damage distribution. The image classification is one of the damage detection techniques and had been applied to the Landsat/TM images (spatial resolution=30m) in the 1995 Kobe earthquake [4]. The applicability of the image classification technique for damage detection using high-resolution satellite image has never discussed in detail. In this paper, the image classification technique is applied to identify the building damage distribution using the post-earthquake QB images based on the observed spectral reflectance characteristics of the surface materials.

II. MEASUREMENT OF SPECTRAL REFLECTANCE

Since the radiation reflected from surface materials is observed in the optical images, such as Landsat/TM, QB, and IKONOS images, it is important to collect the spectral reflectance data by the in-situ observation for applying reliable image classification. We conducted the field survey and measured the spectral reflectance of the surface materials using the handy spectrometer (MS-720 of Eko Instruments Co., Ltd.). In order to grasp the reflectance of building materials, the reflectance of roof tile and brick are observed. We also measured the reflectance of asphalt, vegetation, soil and so on. Figure 2(a) shows the photograph during the observation of surface reflectance. The reflectance is computed from the

irradiance of the target material divided by the irradiance of referenced white plate.

Figure 2(b)-(d) show the observed reflectance of the materials. Horizontal axis indicates the wavelength in nanometer and vertical axis indicates reflectance in percentage. Figure 2(b) represents that the reflectance of brick is high in red band range (600-700nm) while the reflectance of roof tile and asphalt is low in the all ranges. Figure 2(c) shows the comparison of green healthy paddy, yellow unhealthy paddy and dead paddy. A rapid increase in reflectance between visible band and near infrared band is observed for the green paddy, while this characteristic is reduced for the yellow paddy, and it is lost for the dead paddy. These trends are also observed for between healthy leaf and volcanic ash-covered

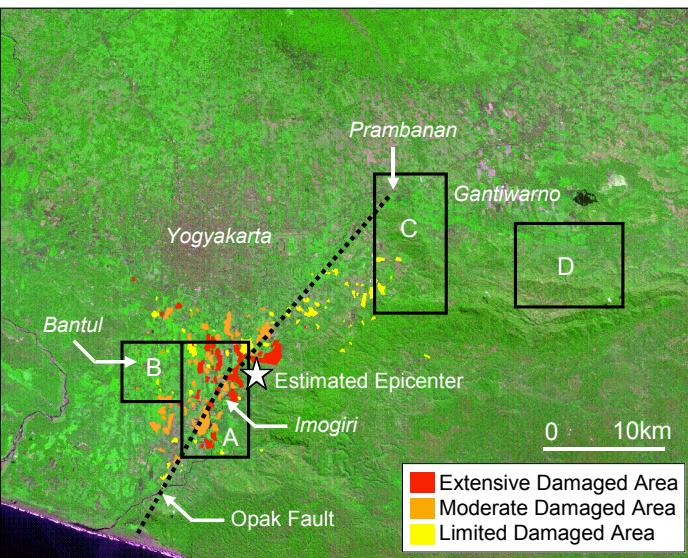


Fig. 1 Coverage of QuickBird images (A-D) and damage distribution estimated by UNOSAT(2006) overlaid on ASTER image.

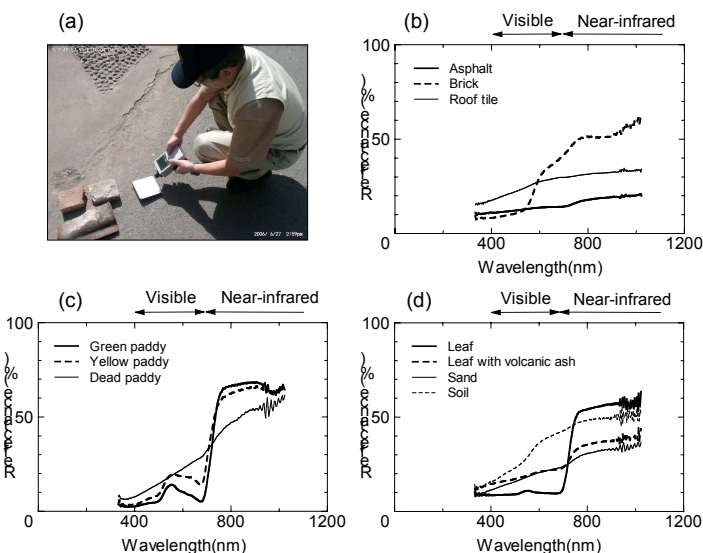


Fig. 2 (a) Observation of surface reflectance. (b)-(d) Reflectance of surface materials.

leaf as shown in Fig. 2(d). The characteristics of dead paddy and ash-covered leaf are similar with those of soil and sand, respectively.

III. DAMAGE ESTIMATION BY IMAGE CLASSIFICATION

In order to identify the distribution of the building damage, post-earthquake QB images are used in this study. The coverage of the QB images is shown by solid squared area (A-D) in Fig. 1. The pan-sharpened images whose spatial resolution is 0.6m are converted from the multi-spectral and panchromatic images using the Brovey transformation [5]. The characteristics of the images are shown in Table 1. The images were observed from June to July 2006. The images of A and B cover the severely damaged areas such as Imogiri and Bantul, respectively. The images of C and D include the area around the Prambanan heritage and Gantiwarno in southern part of Klaten, that are also severely damaged area [3].

The close-ups of the images are shown in Fig. 3. Figure 3(a) represents the completely damaged buildings (top) and undamaged building (bottom) comparing with the pre-event images observed in 2003 and the ground photographs of the building. As shown in the figure, the color of the severely damaged building is turned to white because the bricks of the walls and the debris are exposed on the surface ground. On the other hand, the undamaged building is covered with roof tiles in both of the pre- and post-event images. As shown in Fig. 2, the spectral characteristic of brick is different from that of roof tile. These suggest that it is possible to extract severely damaged area by discriminating the areas covered with bricks from the areas covered with roof tiles.

Table 1 Characteristics of QuickBird images.

Image	Date	Time	Satellite		Sun		Spatial Resolution (m)
			Azimuth (deg.)	Elevation (deg.)	Azimuth (deg.)	Elevation (deg.)	
A	Jun. 13, 2006	AM 10:14	N118E	61	N33E	53	0.6
B	Jun. 8, 2006	AM 10:09	N134E	43	N35E	53	0.6
C	Jun. 13, 2006	AM 10:14	N118E	61	N33E	53	0.6
D	Jul. 7, 2006	AM 10:25	N247E	73	N32E	55	0.6

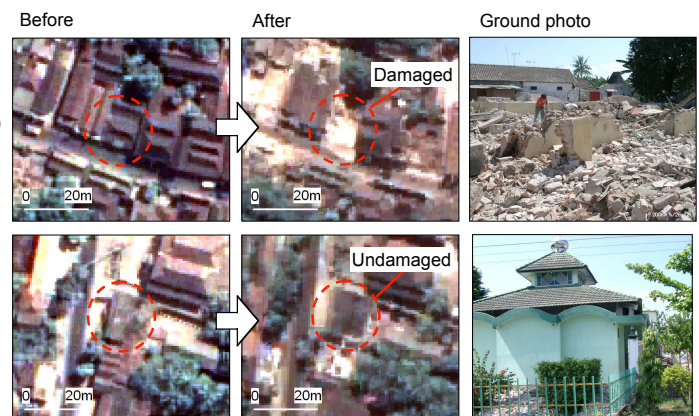


Fig. 3 Comparison of pre-, post-earthquake images and ground photos in severely damaged area and undamaged area.

2007 Urban Remote Sensing Joint Event

The supervised image classification technique is applied to the post-earthquake QB images to identify the damage distribution. The area of the collapsed buildings covered with bricks, undamaged buildings covered with roof tile, vegetation (tree and paddy), bare ground, water of river and so on are extracted for the supervised data of the image classification. About 5,000-10,000 pixels for each material are selected and the maximum likelihood image classification [6] is applied to the images. The time required for the selection of the supervised data and applying the classification is much less than that for the visual interpretation. It means the identification of the damage by the image classification is faster than that by the visual interpretation.

The original QB image and the results of the classification are shown in Fig. 4(a) and (b), respectively. In Fig. 4(b), black pixels indicate bricks classified as collapsed buildings while gray pixels indicate roof tiles classified as undamaged buildings. The close-up of the central part of Imogiri is shown in Fig. 5 that covers the solid squared area in Fig. 4. The pre- and post-earthquake images are also shown in the figure. The comparison between pre- and post-earthquake images reveals that the completely collapsed buildings are covered with the

white materials, such as bricks and debris. In the classified image, they are almost correctly classified as bricks.

In order to identify severely damaged areas, the images are segmented to 100m square meshes and the number of pixels classified as the damaged building in a mesh is computed. Here, ND and NU is defined as the number of pixels classified as damaged building (brick) and undamaged building (roof tile), respectively. In order to avoid the meshes that do not contain settlement area, the meshes that the sum of ND and NU is less than 20% of total pixels in a mesh are eliminated in the analysis. DI (Damage Index) is computed in each mesh based on the following equation.

$$DI = ND / (ND + NU) * 100 \quad (1)$$

Higher DI indicates larger area occupied by severely damaged buildings in the classification. The distribution of DI computed from the classified image (A) are illustrated in Fig. 4(c). The figure shows that high DI area that indicates severely damaged area is widely distributed. The distributions of DI in

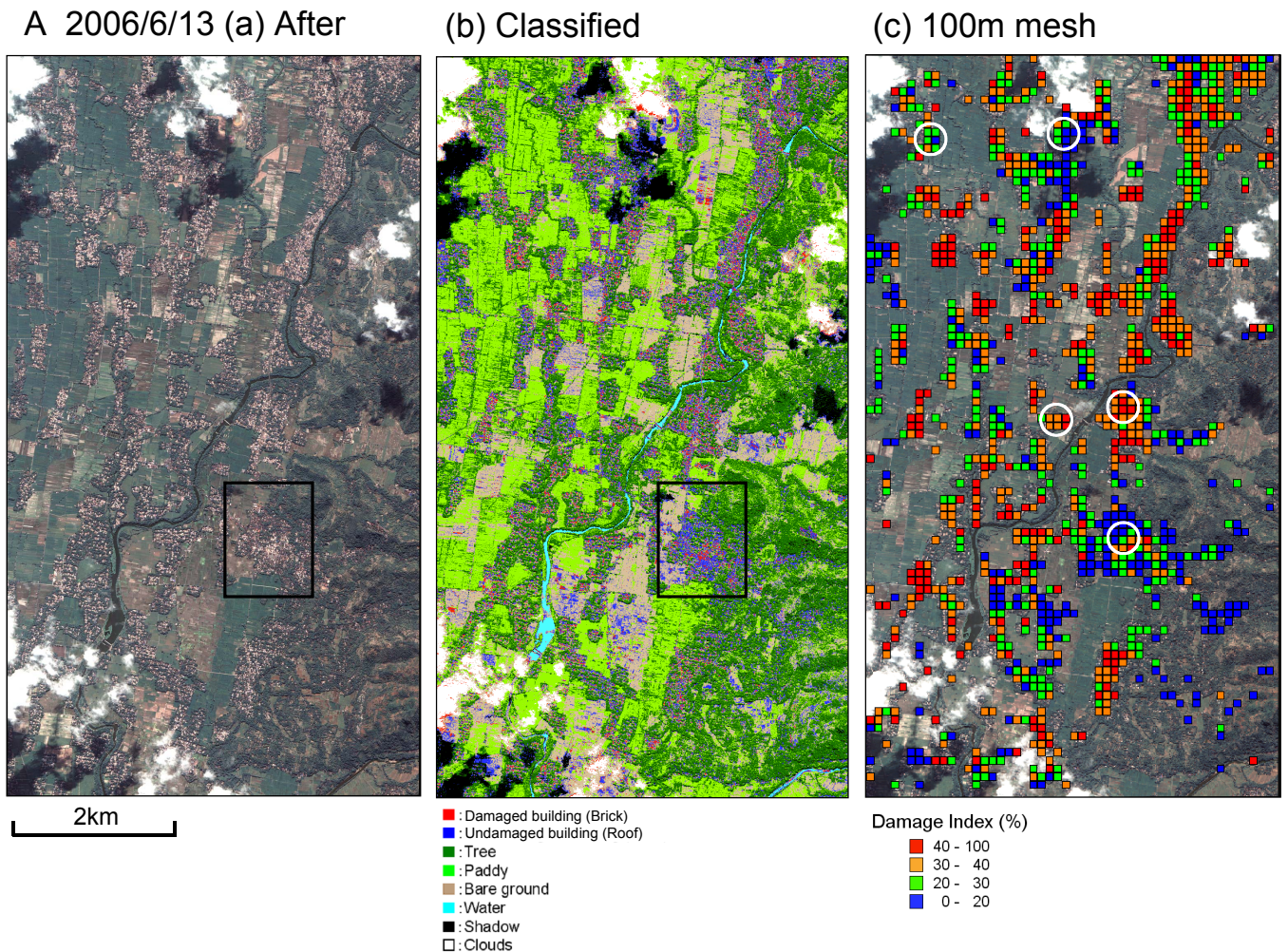


Fig. 4 (a) QuickBird image A, (b) Classified image, (c) Damage distribution estimated from classified image.

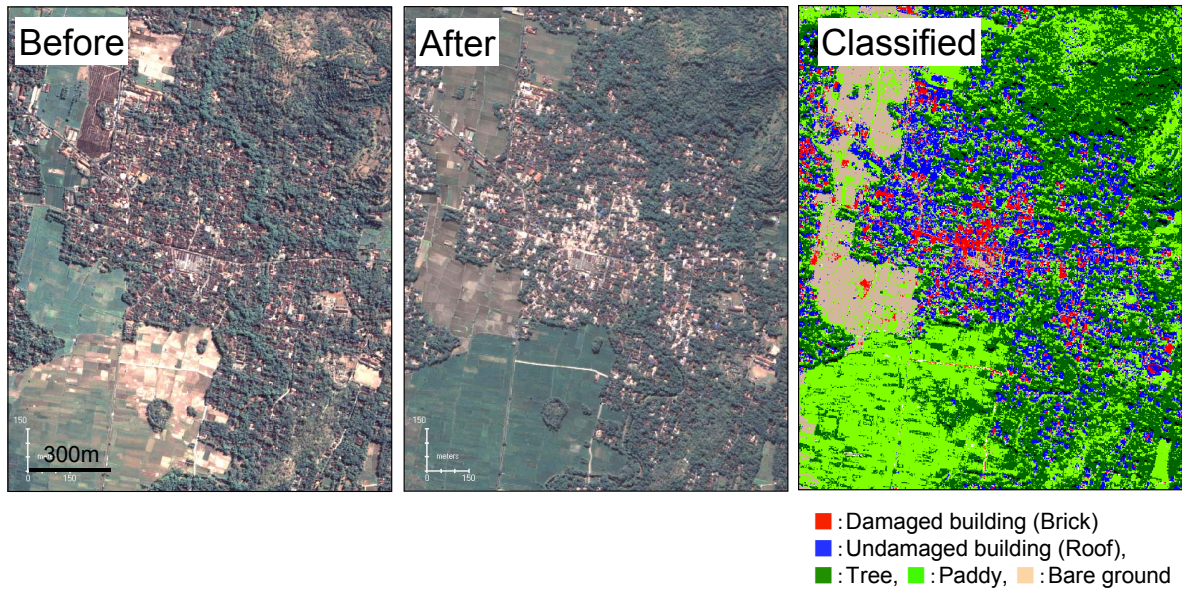


Fig. 5 Comparison between pre-, post-earthquake QB images and classified images.

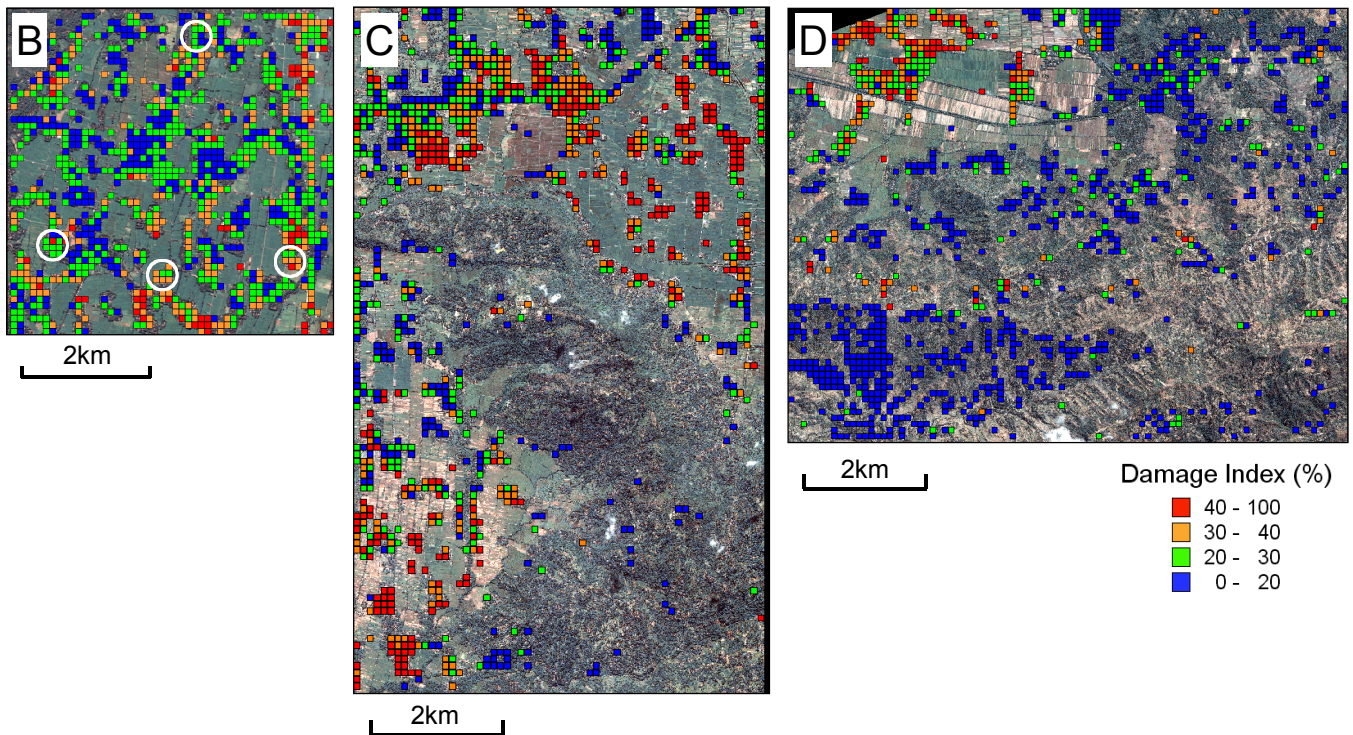


Fig. 6 Estimated damage estimation of image B, C, and D.

the images (B, C, and D) are shown in Fig. 6. As shown in the B image, the damage in the central part of Bantul is not so severe while extensive damage is observed in the southern and eastern area. The estimated damage distribution in Bantul and Imorigi almost agree with the UNOSAT map. The high DI areas are also observed in the northern and southern part of C image and the north-western part of D image. These results

suggest the building damage is also severe in the southern part of Klaten located in relatively far from the epicenter.

IV. COMPARISON WITH DAMAGE STATISTICS

In the epicentral region, such as Bantul and Imogiri, the field survey for building damage was conducted by the Japanese survey team of structural engineers [7]. The open

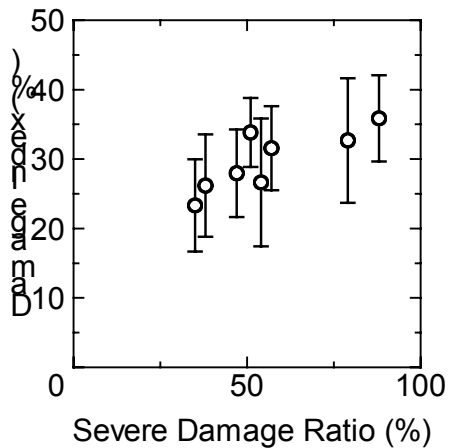


Fig. 7 Comparison between observed damage ratio (severe damage) and damage index computed from classified image

circles in the image A of Fig. 4 and the image B of Fig. 5 indicates the survey points. The centers of the points indicate the locations of the public buildings (schools and town offices) whose damage levels were minutely investigated by the survey team. The damage statistics for the residential houses were also collected in an about 250m radius of the public buildings. The damage level of each building was classified into three categories (Severe, Moderate, and Limited). Approximately from 15 to 60 buildings are investigated in each survey area.

Figure 7 shows the comparison between the damage ratio of severe damaged buildings in the damage statistics and the DI computed from the classified images. Since the survey area covers a dozen of meshes, the averages and their standard deviations of DI are indicated by circle and error bar, respectively. In this figure, as the damage ratio increases, DI also seems to increase, although the standard deviations vary widely. The trend of the computed DI almost agrees with the severe damage ratio. The results show that the image classification technique and the computation of DI are valid for the identification of the building damage. In the future works, the result of the image classification of not only post-earthquake images but also pre-earthquake images would be included in the analysis for more reliable classification.

V. CONCLUDING REMARKS

In this study, the areas damaged by the 2006 Central Java earthquake are identified from the high-resolution satellite

images. Based on the field survey for the spectral reflectance of surface materials, the image classification technique is applied to post-earthquake QuickBird images to detect the areas covered with bricks (damaged buildings) and the areas covered with roof tiles (undamaged buildings). The distribution of the building damage is evaluated by computing Damage Index (DI) from the classified images. The severely damaged areas are distributed not only in Bantul and Imogiri, located near the epicenter, but also in Gantiwarno, the southern part of Klaten located 20-30km away from the epicenter. The distribution of the DI is compared with the damage statistics by the field survey. The result shows that the DI almost agrees with the severe damage ratio. The image classification allows us to analyze the wide-area image quickly compared with the visual interpretation. Although the coverage of the high-resolution satellite images is narrower than that of other optical images, such as Landsat/TM and ASTER images, the detailed damage distribution can be identified if the required images are available.

ACKNOWLEDGMENTS

This study was partially supported by the Ministry of Education, Science, Sports, and Culture, Grant-in Aid for Special Purpose No.1890001 (Representative: Prof. Hiroshi Kawase) and the Center for Urban Earthquake Engineering, Tokyo Institute of Technology. The authors gratefully acknowledge Prof. Yukio Kosugi, Tokyo Institute of Technology for providing one of the QuickBird images.

REFERENCES

- [1] International Charter "Space and Major Disaster", <http://www.disasterscharter.org/>, (last updated December 2006).
- [2] UNOSAT, "Indonesia Maps", <http://unosat.web.cern.ch/unosat/asp/>, (last updated December 2006).
- [3] Murakami, H., Pramitasari, D. and Kawase, H., "Damage Distribution and Seismic Intensity Estimation in the 2006 Central Java Earthquake", *Proceedings of the Annual Conference of the Institute of Social Safety Science*, No.19, 2006, pp.43-46 (in Japanese with English abstract).
- [4] Matsuoka, M., Yamazaki, F. and Midorikawa, S., "Characteristics of Satellite Optical Images in Areas Damaged by the 1995 Hyogo-Ken Nanbu Earthquake", *Journals of the Japan Society of Civil Engineers*, No.668/I-54, 2000, pp.177-185 (in Japanese with English abstract).
- [5] Pohl, C. and Van Genderen, J. L., "Multisensor Image Fusion in Remote Sensing: Concepts, Methods and Applications", *International Journal of Remote Sensing*, Vol.19, No.5, 1998, pp.823-854.
- [6] Takagi, M. and Shimoda, H., "Handbook of Image Analysis (Revised Edition)", University of Tokyo Press, 2004.
- [7] Maeda, T., Kono, S., Sanada, Y. and Takahashi, N., "5.3.3 Damage of Residential Houses, Reconnaissance Report of Building Damage due to the 27 May 2006 Central Java, Indonesia Earthquake", Architectural Institute of Japan, 2007 (in press).